Review

Force–velocity relationships in actin–myosin interactions causing cytoplasmic streaming in algal cells

Haruo Sugi[1],* and Shigeru Chaen[2]

[1]*Department of Physiology, School of Medicine, Teikyo University, Itabashi-ku, Tokyo 173-8605, Japan* and
[2]*Department of Applied Physics, College of Humanities and Science, Nihon University, Setagaya-ku, Tokyo 156-8550, Japan*

*Author for correspondence (e-mail: sugi@med.teikyo-u.ac.jp)

Summary

Cytoplasmic streaming in giant internodal cells of green algae is caused by ATP-dependent sliding between actin cables fixed on chloroplast rows and cytoplasmic myosin molecules attached to cytoplasmic organelles. Its velocity ($\geq 50\ \mu m\ s^{-1}$) is many times larger than the maximum velocity of actin–myosin sliding in muscle. We studied kinetic properties of actin–myosin sliding causing cytoplasmic streaming in internodal cell preparations of *Chara corallina*, into which polystyrene beads, coated with cytoplasmic myosin molecules, were introduced. Constant centrifugal forces directed opposite to the bead movement were applied as external loads. The steady-state

force–velocity (P–V) curves obtained were nearly straight, irrespective of the maximum isometric force generated by cytoplasmic myosin molecules, indicating a large duty ratio of cytoplasmic myosin head. The large velocity of cytoplasmic streaming can be accounted for, at least qualitatively, by assuming a mechanically coupled interaction between cytoplasmic myosin heads as well as a large distance of unitary actin–myosin sliding.

Key words: cytoplasmic streaming, actin–myosin sliding, cytoplasmic myosin, actin cables, centrifuge microscope, *Nitellopsis obtusa*, *Chara corallina*.

Characteristic features of ATP-dependent actin–myosin interaction causing cytoplasmic streaming

Cytoplasmic streaming is widely observed in a variety of plant cells. The mechanism of cytoplasmic streaming has been studied most intensively with giant internodal cells of green algae because of their large size (diameter, approximately 500 μm; length, >10 cm). It is now well established that cytoplasmic streaming is caused by ATP-dependent interaction between well-organized actin filament arrays fixed on the rows of chloroplasts (actin cables) and 'cytoplasmic' myosin molecules attached to amorphous cytoplasmic organelles. The sliding between actin and cytoplasmic myosin results in movement of the organelles in one direction, determined by the polarity of the actin cables, thus causing streaming of the surrounding cytoplasm (Kamiya and Kuroda, 1956; Kamitsubo, 1966; Nagai and Rebhum, 1966; Kersey and Wessels, 1976; Kato and Tonomura, 1977; Nagai and Hayama, 1979; Fig. 1). The direction of cytoplasmic streaming is reversed across the indifferent zone where chloroplasts are absent, reflecting the reversal of actin cable polarity across the indifferent zone. As the two indifferent zones run parallel to the cell's long axis, cytoplasmic streaming rotates longitudinally in the cell.

Although both cytoplasmic streaming and muscle

contraction are caused by ATP-dependent actin–myosin interaction, they differ from each other in some properties. Contraction and relaxation in skeletal muscle is regulated by changes in intracellular Ca^{2+} concentration *via* regulatory proteins on actin filaments (Ebashi and Endo, 1968); a muscle is relaxed at pCa ≥ 7 and fully contracts at pCa ≤ 5. By contrast, cytoplasmic streaming occurs continuously even at pCa ≥ 7 and stops at pCa ≤ 6 (Williamson, 1975; Williamson and Ashley, 1982; Tominaga et al., 1983). Latex beads coated with skeletal muscle myosin slide along actin cables when they are introduced into an internodal cell with Mg-ATP, but the bead movement is insensitive to pCa (Shimmen and Yano, 1984), indicating that regulatory proteins are absent on actin cables, while cytoplasmic myosin is responsible for the Ca^{2+}-induced stoppage of cytoplasmic streaming. Using the centrifuge microscope, Chaen et al. (1995) showed that the Ca^{2+}-induced actin–cytoplasmic myosin linkages are stronger than their rigor linkages, suggesting that a cytoplasmic myosin head can bind with actin at two different sites. Higashi-Fujime et al. (1995) reported that proteolytic cleavage of actin impaired ATP-dependent actin filament sliding on skeletal muscle myosin but not on cytoplasmic myosin, suggesting that cytoplasmic myosin may interact with actin at sites different from those of muscle myosin.
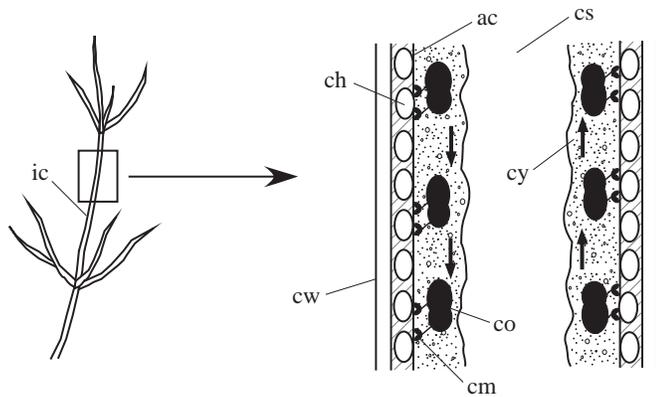
Fig. 1. Diagram of cytoplasmic streaming in the internodal cell of green algae. ac, actin cable; ch, chloroplast; cm, cytoplasmic myosin; co, cytoplasmic organelle; cs, cell sap; cw, cell wall; cy, streaming cytoplasm; ic, internodal cell. Arrows indicate direction of cytoplasmic streaming.

The most striking feature of cytoplasmic streaming is that its velocity ($\geq 50\ \mu m\ s^{-1}$; Kamiya and Kuroda, 1956) is many times larger than the maximum velocity of actin–myosin sliding in muscle (approximately $3\ \mu m\ s^{-1}$; Oiwa et al., 1990). In the presence of Mg-ATP, muscle myosin-coated beads slide on actin cables with velocities similar to the maximum unloaded velocity of actin–myosin sliding in muscle (Sheetz and Spudich, 1983; Oiwa et al., 1990), whereas muscle actin filaments move on cytoplasmic myosin-coated glass surface with velocities similar to those of native cytoplasmic streaming (Higashi-Fujime et al., 1995). These results indicate that it is cytoplasmic myosin that is responsible for the rapid cytoplasmic streaming. Meanwhile, the ultrastructure of cytoplasmic myosin molecules, consisting of two heads connected to one tail, is similar to that of skeletal muscle myosin, except that the tail length is much shorter in the former than in the latter (Yamamoto et al., 1999).

Steady-state force–velocity relationships of ATP-dependent actin–myosin sliding causing muscle contraction and cytoplasmic streaming

To eliminate the gap between the biochemistry of actomyosin in solution and the physiology of contracting muscle, we constructed a centrifuge microscope, consisting of a light microscope, a rotor on which a centrifuge cuvette containing the preparation was mounted and a stroboscopic light source (Fig. 2A). The preparation used was a short segment of the internodal cell of *Nitellopsis obtusa* or *Chara corallina*, into which Mg-ATP solution containing muscle myosin-coated polystyrene beads (diameter, 2.8 μm; specific gravity, 1.3 *g*) were introduced (Fig. 2B). The internodal cell preparation was placed in the cuvette in such a way that its chloroplast rows, along which actin cables ran straight, were parallel to the direction of centrifugal force. As the direction of ATP-dependent bead movement is reversed across the indifferent zone, centrifugal forces directed opposite to the bead movement serve as positive loads, while those in the same direction as the bead movement serve as negative loads (Fig. 2B). The amount of load (**P**) on the bead is given by:

$$\mathbf{P} = \Delta\rho V r\omega^2 , \qquad (1)$$

where $\Delta\rho$ is the difference in density between the bead and the surrounding medium ($0.3\ g\ cm^{-3}$), V is the bead volume
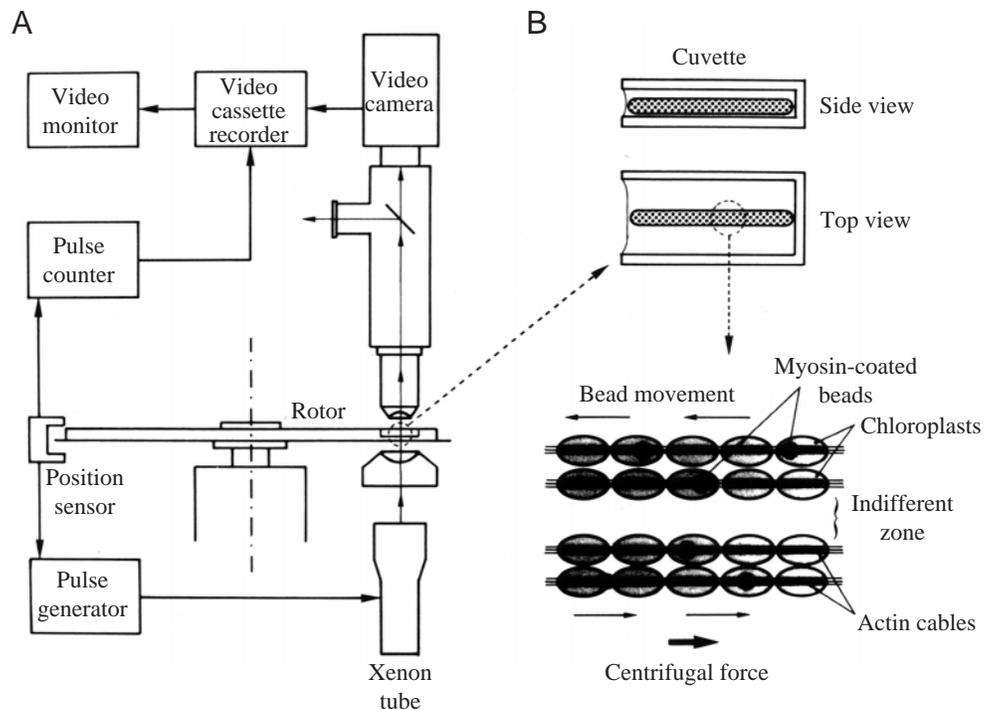

Fig. 2. Centrifuge microscope for studying kinetic properties of ATP-dependent actin–myosin sliding. (A) Diagram showing the centrifuge microscope and video recording system. (B) Application of centrifugal forces serving as positive or negative loads on the beads sliding along actin cables. Reproduced from Oiwa et al. (1990).

($12\ \mu m^3$), *r* is the effective radius of centrifugation (4.5–7 cm) and ω is the angular velocity of the rotor. Further details of the centrifuge microscope system have been described elsewhere (Kamitsubo et al., 1989; Oiwa et al., 1990).

Under a constant centrifugal force serving as a positive load, skeletal muscle myosin-coated beads moved with a constant velocity over a large distance (Fig. 3A), indicating the definite steady-state relationship between the load (=force generated by myosin molecules on the bead) and the velocity of actin–myosin sliding. The maximum unloaded velocity of bead movement ($\mathbf{V}_{max}$) was 1.6–3.6 $\mu m\ s^{-1}$. The bead stopped moving when the load reached the maximum isometric force ($\mathbf{P}_0$) generated by myosin molecules. The force–velocity ($\mathbf{P}$–$\mathbf{V}$) curve obtained was hyperbolic in shape in the low force range but deviated from the hyperbola in the high force range (Fig. 3B). The shape of the $\mathbf{P}$–$\mathbf{V}$ curve was nearly similar to that obtained with tetanized single skeletal muscle fibres (Edman, 1988), indicating tha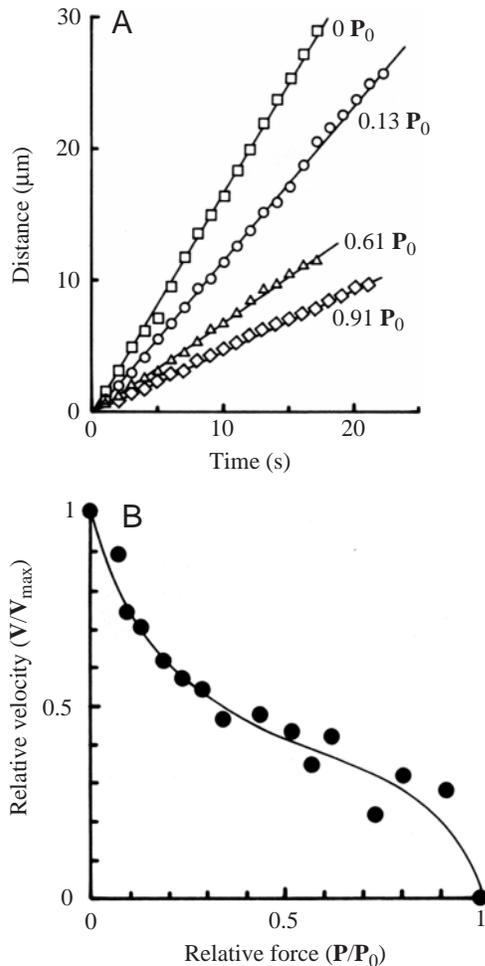t muscle myosin molecules retain their basic kinetic properties of contracting muscle fibres despite their random orientation on the bead (Oiwa et al., 1990).

During the course of the above experiments, we made an incidental observation that, when uncoated beads suspended in Mg-ATP solution were introduced into *Chara* internodal cells, the bead moved along actin cables with velocities and directions similar to those of native cytoplasmic streaming. The beads stopped moving at pCa <6 or by removal of ATP from the surrounding medium. These features of bead movement indicate that it is caused by cytoplasmic myosin molecules, which remain in the cell and attach spontaneously to the bead surface to interact with actin cables. We therefore took the opportunity to determine $\mathbf{P}$–$\mathbf{V}$ characteristics of ATP-dependent actin–myosin sliding causing cytoplasmic streaming with the centrifuge microscope system.

Under a constant centrifugal force serving as a positive load, the beads moved with a constant velocity, indicating the presence of a steady-state $\mathbf{P}$–$\mathbf{V}$ relationship in actin–myosin interaction causing cytoplasmic streaming (Fig. 4A). $\mathbf{V}_{max}$ was 32–61 $\mu m\ s^{-1}$ (mean ± S.D., 46±8.7 $\mu m\ s^{-1}$; *N*=14) at 24–26°C. The beads stopped moving when the load was increased to $\mathbf{P}_0$, which showed a wide variation from 1.0 pN to 13 pN. The $\mathbf{P}$–$\mathbf{V}$ curve constructed from six different beads with large $\mathbf{P}_0$ (8.6–13 pN) was nearly linear (Fig. 4B) in contrast to the hyperbolic $\mathbf{P}$–$\mathbf{V}$ curve of actin–myosin sliding causing muscle contraction (Fig. 3B). Correction of the data points for the viscous drag force against the bead movement did not alter the shape of the $\mathbf{P}$–$\mathbf{V}$ curve (Chaen et al., 1995). The $\mathbf{P}$–$\mathbf{V}$ curve constructed from six different beads with small P_0 (1.0–2.4 pN) was also nearly linear, although the data points showed a large scatter due to difficulties in measuring the velocity of bead movement under small centrifugal forces (Fig. 4C). Despite a large variation of $\mathbf{P}_0$ from 1.0 pN to 13 pN, $\mathbf{V}_{max}$ of the beads with small $\mathbf{P}_0$ values ranged from 36 $\mu m\ s^{-1}$ to 60 $\mu m\ s^{-1}$, indicating that $\mathbf{V}_{max}$ was independent of $\mathbf{P}_0$.

On the other hand, when centrifugal forces in the same direction as the bead movement were applied as negative loads, the velocity of bead movement first decreased under small negative loads and then increased with increasing negative load until the bead was finally detached from the actin cables (Fig. 4D). This puzzling phenomenon has also been seen in actin–skeletal muscle myosin sliding (Oiwa et al., 1990) and microtubule–kinesin sliding (Hall et al., 1993). As the centre of gravity of a polystyrene bead (diameter, 2.8 μm) is 1.4 μm above the actin–myosin contact, substantial torque forces around the bead would compress myosin molecules to inhibit actin–myosin sliding.

Fig. 3. Force–velocity ($\mathbf{P}$–$\mathbf{V}$) characteristics of ATP-dependent actin–myosin sliding in muscle contraction. (A) Constant velocity sliding of a skeletal muscle myosin-coated bead along actin cables under four different positive loads, expressed relative to maximum isometric force ($\mathbf{P}_0$). (B) Typical example of a steady-state $\mathbf{P}$–$\mathbf{V}$ curve of actin–myosin sliding. Reproduced from Oiwa et al. (1990).

Kinetic properties of cytoplasmic actin–myosin interaction causing cytoplasmic streaming

The Hill equation (Hill, 1938), describing the relationship between the load (=force; $\mathbf{P}$) and the velocity of actin–myosin sliding ($\mathbf{V}$) can be written as:

$$(\mathbf{P} + a)\mathbf{V} = b(\mathbf{P}_0 - \mathbf{P}) , \qquad (2)$$

where a and b are constants corresponding to two asymptotes of a rectangular hyperbola. $\mathbf{P}=\mathbf{P}_0$ when $\mathbf{V}=0$, and $\mathbf{V}=\mathbf{V}_{max}$ when $\mathbf{P}=0$. The value of $\mathbf{P}_0$ is taken as the maximum number of myosin molecules generating actin–myosin sliding, while $\mathbf{V}_{max}$ is thought to reflect the maximum cycling rate of ATP-dependent actin–myosin interaction. The value of $a/\mathbf{P}_0$ is a measure of curvature of the $\mathbf{P}$–$\mathbf{V}$ curve; the larger $a/\mathbf{P}_0$ is, the less pronounced is the curvature of the $\mathbf{P}$–$\mathbf{V}$ curve. It is suggested that a large value of $a/\mathbf{P}_0$ is associated with a low efficiency, with which chemical energy derived from ATP hydrolysis is converted into mechanical work (Woledge, 1968). Although the straight $\mathbf{P}$–$\mathbf{V}$ curve of actin–cytoplasmic myosin sliding cannot be fitted to the Hill equation with reasonable accuracy, the large $a/\mathbf{P}_0$ value suggests a very low

efficiency of chemo-mechanical energy conversion in ATP-dependent actin–myosin interaction causing cytoplasmic streaming.

The minimum value of $\mathbf{P}_0$ generated by cytoplasmic myosin molecules on the bead was 1.0 pN, which is smaller than the reported values of force spikes of single muscle myosin molecules (1–7 pN, Finer et al., 1994; 5–6 pN, Ishijima et al., 1994, 1996). In our experiments, however, the forces measured are time-averaged values against continuously applied centrifugal forces and do not contradict reported values of transient force spikes. On this basis at least, a few myosin molecules may be involved even in generating a $\mathbf{P}_0$ of 1 pN if random orientation of myosin molecules on the bead is taken into consideration. On the other hand, the large $\mathbf{V}_{max}$ in
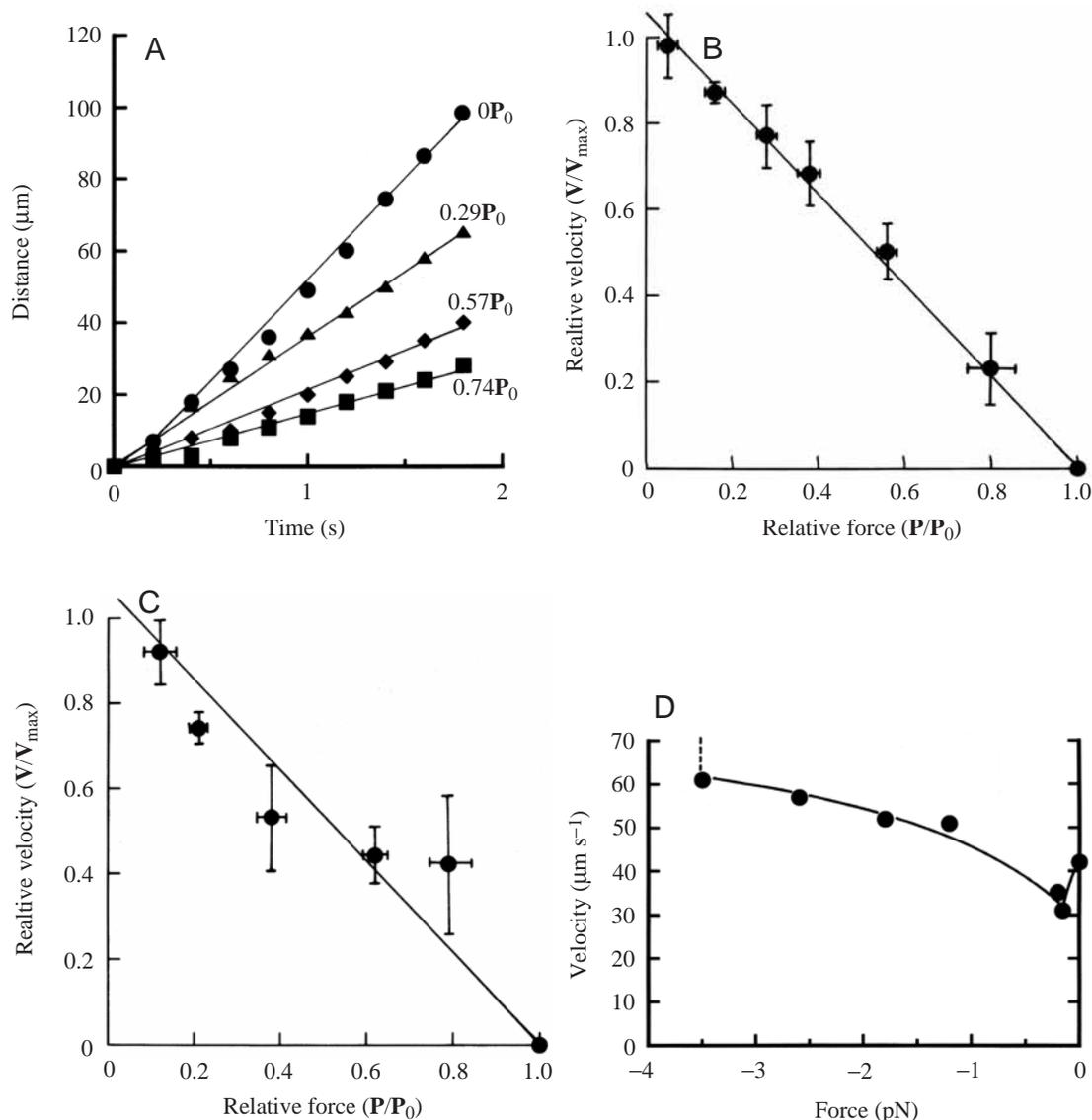

Fig. 4. Force–velocity ($\mathbf{P}$–$\mathbf{V}$) characteristics of ATP-dependent actin–myosin sliding causing cytoplasmic streaming. (A) Constant velocity sliding of a cytoplasmic myosin-coated bead along actin cables under different positive beads. (B) $\mathbf{P}$–$\mathbf{V}$ curve constructed from six different beads with large (8.6–13 pN) maximum isometric force ($\mathbf{P}_0$). (C) $\mathbf{P}$–$\mathbf{V}$ curve constructed from six different beads with small (1.0–2.4 pN) maximum isometric force ($\mathbf{P}_0$). Data points in the $\mathbf{P}$–$\mathbf{V}$ curves represent mean values, with vertical and horizontal bars indicating S.D. (N=6). (D) $\mathbf{P}$–$\mathbf{V}$ curve for the movement of a bead under negative loads, expressed in pN.

actin–cytoplasmic myosin sliding indicates a large cycling rate of actin–cytoplasmic myosin interaction. Contrary to this expectation, however, the actin-activated ATPase activity of *Chara* cytoplasmic myosin in solution is similar to that of muscle myosin (Tanimura and Higashi-Fujime, in press). This paradox will be considered later.

In the Huxley contraction model (Huxley, 1957), in which actin and myosin exhibit repeating attachment–detachment cycles, each coupled with ATP hydrolysis, the probability that all myosin heads are detached from actin ($\mathbf{P}_{off}$) is written as:

$$\mathbf{P}_{off} = (1 - p)^n , \qquad (3)$$

where p is the fraction of time in which a myosin head firmly attaches to actin in one actin–myosin interaction cycle and is called the duty ratio (Howard, 1997), while n is the number of myosin heads. $\mathbf{P}_{off}$ is negligible for large numbers of n but becomes substantial for small numbers of n, especially if the value of p is small. During the period of $\mathbf{P}_{off}$, the bead is pulled back (or does not go forward) under applied centrifugal forces opposing the bead movement. The resulting zigzag bead movement would considerably reduce $\mathbf{V}_{max}$. In fact, the value of $\mathbf{V}_{max}$ was reduced with decreasing values of $\mathbf{P}_0$ in actin–skeletal muscle myosin sliding, resulting in a less pronounced hyperbolic part of the $\mathbf{P}$–$\mathbf{V}$ curve in the low force range (Oiwa et al., 1990). The value of $\mathbf{V}_{max}$ did not, however, decrease with decreasing $\mathbf{P}_0$ values in actin–cytoplasmic myosin sliding, indicating that cytoplasmic myosin heads have a large duty ratio. As the number of cytoplasmic myosin attached to each cytoplasmic organelle is expected to be small, their large duty ratio is essential to continuously move cytoplasmic organelles along actin cables. If at least two cytoplasmic myosin molecules are assumed to be necessary for continuous bead movement on actin, the duty ratio for each of the four myosin heads, working independently of each other, is at least 0.25.

Possible mechanism producing the rapid cytoplasmic streaming

Based on the concept of duty ratio, there are three basic kinetic factors of myosin determining the maximum velocity of actin–myosin sliding ($\mathbf{V}_{max}$; Howard, 1997). These factors are (1) duty ratio of myosin head (p), (2) ATPase rate per myosin head (A) and (3) unitary sliding distance produced by myosin head (d). The value of p is written as:

$$p = (d \times A) / \mathbf{V}_{max} . \qquad (4)$$

In ATP-dependent actin–myosin interaction in skeletal muscle, p is approximately 0.05 (Uyeda et al., 1990; Finer et al., 1994), A is approximately 20 s^{-1} head^{-1} (Toyoshima et al., 1987) and $\mathbf{V}_{max}$ is approximately 3 µm s^{-1} (Oiwa et al., 1990). Putting these values into equation 4, we obtain a d of approximately 8 nm, a value consistent with the contraction model, in which unitary actin–myosin sliding is produced by rotation of myosin heads (Huxley and Simmons, 1971). The small duty ratio in skeletal muscle myosin heads implies

that at least 20 heads, working together, are necessary for continuous actin–myosin sliding.

In ATP-dependent actin–myosin interaction in cytoplasmic streaming, on the other hand, p is assumed to be 0.25, while $\mathbf{V}_{max}$ is approximately 50 µm s^{-1} (Chaen et al., 1995). The value of d is at present unknown but, on the basis of the Huxley–Simmons scheme, it is constrained by the size of the myosin head and may not be more than about 20 nm. In order to make d realistic ($\leq$20 nm), it follows from equation 3 that A should be approximately 425 s^{-1} head^{-1}. This extremely high cycling rate of actin–myosin interaction, which is likely to be associated with a very low efficiency of chemo-mechanical energy conversion, is consistent with the very large value of $a/\mathbf{P}_0$ of the straight $\mathbf{P}$–$\mathbf{V}$ curve (Fig. 4B,C; Chaen et al., 1995). This idea, however, contradicts the result that the actin-activated ATPase rate of cytoplasmic myosin in solution is similar to that of skeletal muscle myosin (20 s^{-1} head^{-1}; Tanimura and Higashi-Fujime, in press). This paradox may be solved at least qualitatively in the following way. In the movement of cytoplasmic organelles or cytoplasmic myosin-coated beads along actin filaments, there seems to be a mechanically coupled interaction between the heads of myosin molecules attached to the same bead. Such interactions are absent in solutions where myosin molecules diffuse freely. Due to its large value of p, each cytoplasmic myosin head interacting with actin would have many chances of being 'pushed forward' by sliding forces generated by the head(s) of other myosin molecules attached to the same bead. When a head interacting with actin is pushed forward, it would immediately be detached from actin to restart its sliding force generation. This would considerably reduce the time of attachment of each myosin head to actin without changing its duty ratio and would therefore result in a marked increase in its ATPase rate compared with that in solution.

The above idea of the mechanically coupled myosin head interaction comes from the report that, in single tetanized skeletal muscle fibres, the value of $\mathbf{V}_{max}$ measured by the slack test increases more than twofold in the presence of a small resting tension ($\leq$7% of $\mathbf{P}_0$) at a sarcomere length of approximately 3 µm (Edman, 1988). In the slack test, a tetanized fibre is subjected to a quick release of up to 30% of the initial fibre length. As the resting tension decreases steeply to a negligible value with decreasing sarcomere length for the first approximately 6% of sarcomere shortening following release, this indicates that the effect of resting tension to compress the stretched sarcomere (and therefore to push the myosin heads attached to actin forward) is only transient. This implies that if a myosin head is pushed forward by a transient force, the rate of actin–myosin interaction coupled with ATP hydrolysis can be markedly increased.

Meanwhile, the increase of A (from 20 s^{-1} head^{-1} to 425 s^{-1} head^{-1}) by the mechanically coupled myosin head interaction can be reduced if the value of d is not actually constrained by the size of the myosin head and could be as large as approximately 100 nm by a biased Brownian ratchet mechanism (Vale and Oosawa, 1990). In this case, the increase

of A is reduced from $20\ \mathrm{s^{-1}\ head^{-1}}$ to approximately $85\ \mathrm{s^{-1}\ head^{-1}}$. Much more experimental work is necessary to further understand the mechanisms of cytoplasmic streaming. In the Huxley contraction model (Huxley, 1957), the value of V_{max} is determined by the balance between positive forces generated by myosin heads and negative forces due to negative strain of myosin heads. If cytoplasmic myosin heads are assumed to detach from actin without generating appreciable negative strain forces, this would also result in a marked increase in the velocity of actin–myosin sliding in cytoplasmic streaming compared with that in muscle contraction. The myosin head negative strain is not explicitly taken into consideration in the concept of duty ratio but is implicitly included in the value of d, and in this sense d may not necessarily be constrained by the size of the myosin head.

References

Chaen, S., Inoue, J. and Sugi, H. (1995). The force–velocity relationship of the ATP-dependent actin–myosin sliding causing cytoplasmic streaming in algal cells, studied using a centrifuge microscope. *J. Exp. Biol.* **198**, 1021-1027.

Ebashi, S. and Endo, M. (1968). Calcium ion and muscle contraction. *Prog. Biophys. Mol. Biol.* **18**, 125-183.

Edman, K. A. P. (1979). The velocity of unloaded shortening and its relation to sarcomere length. *J. Physiol. Lond*. **291**, 143-159.

Edman, K. A. P. (1988). Double-hyperbolic force–velocity relation in frog muscle fibres. *J. Physiol. Lond*. **494**, 301-321.

Finer, J. T., Summons, R. M. and Spudich, J. A. (1994). Single myosin molecule mechanics: piconewton forces and nanometre steps. *Nature* **368**, 113-119.

Hall, K., Cole, D. G., Yen, Y., Scholey, J. M. and Baskin, R. J. (1993). Force–velocity relationships in kinesin-driven motility. *Nature* **364**, 457-459.

Higashi-Fujime, S., Ishikawa, R., Iwasawa, H., Kagami, O., Kurimoto, E., Kohama, K. and Hozumi, T. (1995). The fastest actin-based motor protein from the green algae, *Chara*, and its distinct mode of interaction with actin. *FEBS Lett*. **375**, 151-154.

Hill, A. V. (1938). The heat of shortening and the dynamic constants of muscle. *Proc. R. Soc. Lond. B. Biol. Sci.* **126**, 136-195.

Howard, J. (1997). Molecular motors: structural adaptations to cellular functions. *Nature* **389**, 561-567.

Huxley, A. F. (1957). Muscle structure and theories of contraction. *Prog. Biophys. Biophys. Chem*. **7**, 255-318.

Huxley, A. F. and Simmons, R. M. (1971). Proposed mechanism of force generation in striated muscle. *Nature* **233**, 533-538.

Ishijima, A., Harada, Y., Kojima, H., Funatsu, T., Higuchi, H. and Yanagida, T. (1994). Single-molecule analysis of the actomyosin motor using nano-manipulation. *Biophys. Biophys. Res. Commun.* **199**, 1057-1063.

Ishijima, A., Kojima, H., Higuchi, H., Harada, Y., Funatsu, T. and Yanagida, T. (1996). Multiple- and single-molecule analysis of the actomyosin motor by nanometer-piconewton manipulation with a microneedle; unitary steps and forces. *Biophys. J.* **70**, 383-400.

Kamitsubo, E. (1966). Motile protoplasmic fibrils in cells of *Characeae* II. Linear fibrillar structure and its bearing on protoplasmic streaming. *Proc. Jpn. Acad.* **42**, 640-643.

Kamitsubo, E., Ohashi, Y. and Kikuyama, M. (1989). Cytoplasmic streaming in internodal cells of *Nitella* under centrifugal acceleration: a study done with a newly constructed centrifuge microscope. *Protoplasma* **152**, 148-155.

Kamiya, N. and Kuroda, K. (1956). Velocity distribution of the protoplasmic streaming in *Nitella* cells. *Bot. Mag*. **69**, 544-554.

Kato, T. and Tonomura, Y. (1977). Identification of myosin in *Nitella flexilis*. *J. Biochem*. **82**, 777-782.

Kersey, Y. M. and Wessels, N. K. (1976). Localization of actin filaments in internodal cells of *Characean* algae. *J. Cell Biol*. **68**, 264-275.

Nagai, R. and Hayama, T. (1979). Ultrastructure of the endoplasmic factor responsible for cytoplasmic streaming in *Chara* internodal cells. *J. Cell Sci.* **36**, 121-136.

Nagai, R. and Rebham, L. (1966). Cytoplasmic microfilaments in streaming *Nitella* cells. *J. Ultrastruct. Res.* **14**, 571-589.

Oiwa, K., Chaen, S., Kamitsubo, E., Shimmen, T. and Sugi, H. (1990). Steady-state force–velocity relation in the ATP-dependent sliding movement of myosin-coated beads on actin cables *in vitro*. *Proc. Natl. Acad. Sci. USA* **87**, 7893-7897.

Sheetz, M. P. and Spudich, J. A. (1983). Movement of myosin-coated fluorescent beads on actin cables *in vitro*. *Nature* **303**, 31-35.

Shimmen, T. and Yano, M. (1984). Active sliding movement of latex beads coated with skeletal muscle myosin on *Chara* actin bundles. *Protoplasma* **121**, 132-137.

Tanimura, A. and Higashi-Fujime, S. (2002). Characteristic motility of *Chara* myosin. *J. Muscle Res. Cell Motil.* **23**, 185.

Tominaga, Y., Shimmen, T. and Tazawa, M. (1983). Control of cytoplasmic streaming by extracellular Ca^{2+} in permeabilized *Nitella* cells. *Protoplasma* **116**, 75-77.

Toyoshima, Y. Y., Kron, S. J., McNally, E. M., Niebling, K. R., Toyoshima, C. and Spudich, J. A. (1987). Myosin subfragment-1 is sufficient to move actin filaments *in vitro*. *Nature* **328**, 536-539.

Toyoshima, Y., Kron, S. J. and Spudich, J. A. (1990). The myosin step size. *Proc. Natl. Acad. Sci. USA* **87**, 7130-7134.

Uyeda, T. Q. P., Kron, S. J. and Spudich, J. A. (1990). Myosin step size estimation from slow sliding movement of actin over low densities of heavy meromyosin. *J. Mol. Biol.* **214**, 699-710.

Vale, R. D. and Oosawa, F. (1990). Protein motors and Maxwell's demons: does mechanochemical transduction involve a thermal rachet. *Adv. Biophys.* **26**, 97-134.

Williamson, R. E. (1975). Cytoplasmic streaming in *Chara*: a cell model activated by ATP and inhibited by cytochalasin B. *J. Cell Sci.* **17**, 655-668.

Williamson, R. E. and Ashley, C. C. (1982). Free Ca^{2+} and cytoplasmic streaming in the alga *Chara Nature* **296**, 647-651.

Woledge, R. C. (1968). The energetics of tortoise muscle. *J. Physiol. Lond.* **197**, 685-707.

Yamamoto, K., Hamada, S. and Kashiyama, T. (1999). Myosins from plants. *Cell. Mol. Life Sci.* **56**, 227-232.